

Coupled Electromechanical Analysis of a Permanent-Magnet Bearing

Vincenzo Di Dio¹ and Luca Sani²

¹DEIM, Department of Energy, Engineering Information and Mathematical Model
University of Palermo, Palermo, 90128, Italy
vincenzo.didio@unipa.it

²DESTEC, Department of Energy, Systems, Territory and Constructions Engineering
University, Pisa, 56122, Italy
luca.sani@unipi.it

Abstract — In this paper we present a new Permanent Magnets (PMs) bearing, which is composed of a rotor capable to levitate at a short distance from a dedicated stator. Proper configurations of PMs arranged on both the stator and the rotor allows having the magnetic suspension. Intrinsic mechanical instability characterizes the device; a passive stabilization is attempted exploiting eddy currents on a conducting sheet that surrounds the magnets on the stator. The system has been simulated by means of a dedicated numerical code that takes into account the effects of magneto-mechanical coupling. The coupled problem has been integrated by means of a prediction-correction nested scheme. Some interesting results, extensively discussed here, has been produced by simulation activity. In particular the stability of to the center of mass with respect to the translations has been passively obtained, if the rotations are actively prevented.

Index Terms — Computational electromagnetic, coupled analysis, magnetic bearings, magnetic levitation, permanent magnets.

I. INTRODUCTION

In the late 1960s, the modern development of Magnetic Levitation systems (known as MAGLEV) started when the possibility to use magnetic forces to levitate vehicles became sustainable, mainly due to some discoveries of that time: development of low-temperature superconducting wire, transistor and chip based electronic control technology [1], [2]. MAGLEV provides high-speed motion, safety, reliability, low environmental impact and minimum maintenance [3]. There are two basic options to obtain magnetic levitation: a) electromagnetic system [4]-[6] working in attraction mode with forces generated by electromagnets; b) electrodynamic system [7], [8] working in repulsive mode with forces generated by superconductive coils. An application example is flywheel energy storage systems, which are considered to be an attractive alternative to

conventional electrochemical batteries [9], [10]. Unstable behavior is the main feature of both solutions. The first option is unstable in the levitating direction which is vertical, in general. The attractive force increases when the two parts of the system approach each other. The second option, i.e., the electrodynamic system is unstable in the transverse-to-levitation and in the motion directions. Nowadays a new class of MAGLEV systems can be conceived via the use of Rare Earth PMs (e.g., NdFeB) characterized by high values of remnant field. The suspension is then assured by the repulsion of properly shaped PMs [11], [12]. Stability of levitation systems based on PMs is prevented by Earnshaw's theorem [13]. This theorem states that a set of steady charges, magnetizations or currents cannot stay in stable equilibrium under the action of steady electric and magnetic field. As applications of MAGLEV or magnetic bearing devices must be fail-safe, severe constraints are posed on the design and operation of the stabilization systems. So a great effort is devoted to the design of passive and more reliable stabilization devices. In some cases, electric and magnetic systems can avoid the consequences of the Earnshaw's theorem: time varying fields (e.g., eddy currents, alternating gradient), ferrofluids, superconductors and diamagnetic systems. In this paper, the use of eddy current stabilization to reduce or compensate the intrinsic instability of the bearing is investigated: if some magnetized parts of a system are in motion near conductive materials, eddy currents are induced and the system is not under the action of steady magnetic fields. Since the system is now governed by the diffusion equation, the hypothesis of the Earnshaw's theorem (direct consequence of the Laplace equation) is not valid. Some preliminary results of the coupled electromechanical analysis of a PMs bearing are discussed in this paper, demonstrating how the presence of motional induced eddy currents have a positive effect on the dynamic of the bearing device. This electrodynamic effect allows to reduce the complexity of the control

system. Section 2 introduces the proposed device, Section 3 briefly describes the numerical code used for the analysis of the device, while Section 4 discusses the results.

II. PROPOSED DEVICE

The proposed system is shown in Figs. 1 and 2: it exploits the induced eddy currents to contrast the instability related to the PMs arrangement.

It is mainly composed of a toroidal stator and a segmented rotor made of at least three blocks equally spaced along the circumference. The rotor can move with 6 degrees of freedom (DOF) with respect to the fixed stator. The PMs in both the stator and the rotor are arranged in Halbach array configurations [14] focusing the field lines in the airgap between them. A sheet of conductive material surrounds the stator (black in Fig. 2). Levitation along z-direction is achieved by the repulsion of PMs with opposite magnetization. To describe the dynamics of the proposed device we assume that the moving part rotates around a vertical shaft, directed as the z-axis that is the symmetry axis of the stator. Motion-induced eddy currents flow on the stator sheet; subsequently a levitation force on the z-axis in addition with the levitation force of the PMs and a magnetic drag torque are observed. Those currents interact with the PMs of the rotor reducing the cause which produces the eddy currents themselves. This reduction is produced by a drag force on the rotor which produces a velocity reduction, and by moving away the field source (the PMs on the rotor) from the conductive region.

Since the levitation force is a decreasing function of the distance, the system is stable in the levitation direction. When the system rotates in the symmetric configuration, the radial forces are deleted. A net force in the radial direction is expected to appear if the system does not run in symmetrical conditions (e.g., a radial displacement of the rotation shaft occurs). This force is the resultant of the forces between the two PMs systems and of the interactions between the motion-induced eddy currents on the stator and the PMs on the rotor. Earnshaw's theorem states that the forces between the PMs are destabilizing. If we consider a displacement of the rotor in the x-axis (Fig. 2), currents induced on the conductive sheet are stronger on the side of the displacement, while they get weaker on the opposite side where the distance is greater. The net resulting force is then directed along the negative x-axis direction and it performs a stabilizing action. This stabilizing effect occurs in principle also in the case of angular displacement of the rotation shaft with respect to the vertical (y-axis) direction. As a result of this angular displacement, since the rotor is divided in three sectors (or more), some of these sectors are closer to the stator, while others are more distant. The induced currents on the part of the

stator corresponding to the nearest rotor sectors are more intense and the resulting forces exerted on the rotor PMs are stronger. On the contrary, the forces on the more distant rotor sectors are weaker. The final effect is a torque restoring the vertical position of the rotation shaft.

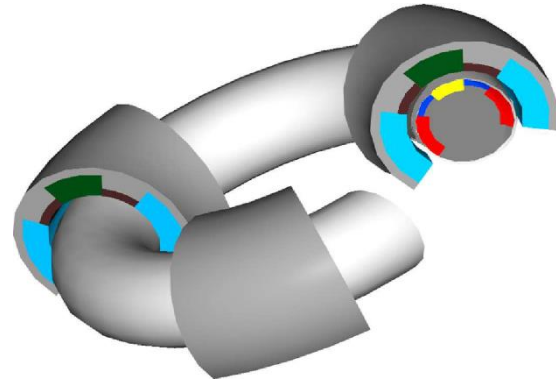


Fig. 1. A 3D view of the analysed device.

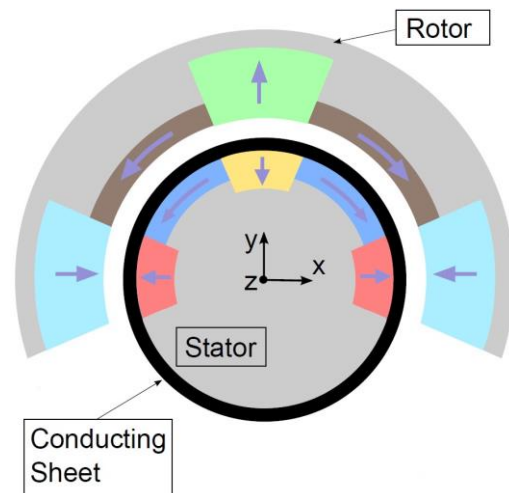


Fig. 2. Cross section of the bearing.

III. THE NUMERICAL FORMULATION

The performances of this device have been investigated by a numerical model. The equations describing the rotor dynamics with six DOFs are inherently nonlinear because of the dependence of the force on the position of the rotor itself. Moreover the problem of rigid body dynamics is coupled with the diffusion equation of the magnetic field. The solution of the electromagnetic problem has been carried out by an integral formulation that reduces the diffusion equation to an equivalent network with time varying parameters. The values of the parameters in the electrical equations are function of the position of the rotor. The details of the adopted formulation are reported in [15] - [23].

Under the hypothesis of linear magnetisable materials, the equations of the problem produced by

the equivalent network formulation coupled with the Newton-Euler equations of motion can be written as:

$$\begin{aligned} \mathbf{L}(C(t))\frac{d\mathbf{i}}{dt} + [\mathbf{R}(C(t)) + \mathbf{K}(C(t), \dot{C}(t))] \mathbf{i} &= \mathbf{e}(t) \\ \mathbf{F}(C(t)) &= m\ddot{\mathbf{q}} \\ \mathbf{M}(C(t)) &= \mathbf{I}_{\theta\theta}\dot{\omega} + \omega \times \mathbf{I}_{\theta\theta}\omega, \end{aligned} \quad (1)$$

where $\mathbf{e}(t)$ represents the vector of the applied voltage generators and \mathbf{i} is the vector of the currents in the elementary volumes, including the equivalent magnetization currents. All the coefficients matrices are function of $C(t)$ which represents the system configuration at the instant t . $C(t)$ is defined as the set of the positions and orientations of all the elementary volumes in which the device is discretized:

$$C(t) = (x(t), y(t), z(t), \phi(t), \theta(t), \psi(t)), \quad (2)$$

$\mathbf{L}(C(t))$ denotes the inductance matrix; $\mathbf{R}(C(t))$ is the resistance matrix and $\mathbf{K}(C(t), \dot{C}(t))$ takes into account the electromotive force due to the motional effects. In particular $\dot{C}(t)$, termed as the derivatives of the system configuration at the instant t , describes the velocity of every elementary volume in the hypothesis of rigid body. The $\dot{C}_i(t)$ corresponding to the i -th elementary volume is constituted by the three components of the translation velocity, the three components of the angular velocity, and the three coordinates of the center of rotation.

Equation (1) is solved by a prediction correction nested scheme. The rationale behind it is the search for an approximation inside the time step of the behaviour of the coefficients in electrical and mechanical equations. The predictor-corrector approach is used to obtain an approximate behavior of the named quantities by a linear interpolation between the known values at the previous time step and the predicted values at the next time step. Inserting this knowledge in the equations has the effect of considering updated values of the coefficients, allowing a coupling between the equations which is stronger than the one in a simply staggered scheme and comparable with a monolithic approach.

The integration algorithm can be described as follows ($\Delta t = t_{n+1} - t_n$):

- assuming $C(t)$ constant in the interval Δt an estimate of the currents at t_n is obtained by a trapezoidal rule applied on (1a);
- an estimate of $C(t_{n+1}) = C_{n+1}$ is obtained by applying forward Euler integration to (1b) and (1c);
- a piecewise linear approximation is assumed for \mathbf{L} in Δt , similarly for \mathbf{R} and \mathbf{K} :

$$\dot{\mathbf{L}}(t_n) \approx \frac{\mathbf{L}(\tilde{C}(t_{n+1})) - \mathbf{L}(\tilde{C}(t_n))}{\Delta t}, \quad (3)$$

and as a consequence,

$$\mathbf{L}(t) \approx \mathbf{L}(t_n) + \dot{\mathbf{L}}(t_n) \cdot (t - t_n) = \mathbf{L}_n + \dot{\mathbf{L}}_n \cdot (t - t_n), \quad (4)$$

similarly for the other coefficients.

- The expressions are introduced in (1a):

$$\begin{aligned} (\mathbf{L}_n + \dot{\mathbf{L}}_n \cdot (t - t_n)) \frac{d\mathbf{i}}{dt} + [(\mathbf{R}_n + \dot{\mathbf{R}}_n \cdot (t - t_n)) + \\ (\mathbf{K}_n + \dot{\mathbf{K}}_n \cdot (t - t_n))] \mathbf{i} = \mathbf{e}(t) \quad t \in [t_n, t_{n+1}]. \end{aligned} \quad (5)$$

- Integrating with a trapezoidal-like rule we obtain the corrected values of the currents at the instant t_{n+1} . We write:

$$\int_{t_n}^{t_{n+1}} (\mathbf{L}_n + \dot{\mathbf{L}}_n \cdot (t - t_n)) \frac{d\mathbf{i}}{dt} + \int_{t_n}^{t_{n+1}} [(\mathbf{R}_n + \dot{\mathbf{R}}_n \cdot (t - t_n)) + (\mathbf{K}_n + \dot{\mathbf{K}}_n \cdot (t - t_n))] \mathbf{i} dt = \int_{t_n}^{t_{n+1}} \mathbf{e}(t), \quad (6)$$

- and after the numerical integration:

$$\begin{aligned} \mathbf{L}_n(\mathbf{i}_{n+1} - \mathbf{i}_n) + \frac{\Delta t \dot{\mathbf{L}}_n}{2}(\mathbf{i}_{n+1} + \mathbf{i}_n) + \frac{\Delta t(\mathbf{R}_n + \mathbf{K}_n)}{2}(\mathbf{i}_{n+1} + \mathbf{i}_n) + \\ + \frac{\Delta^2 t(\dot{\mathbf{R}}_n + \dot{\mathbf{K}}_n)}{2} \mathbf{i}_{n+1} = \frac{\Delta t(\mathbf{e}_{n+1} + \mathbf{e}_n)}{2}. \end{aligned} \quad (7)$$

- Collecting terms finally gives a linear system where the unknowns are the corrected currents at the instant t_{n+1} :

$$\begin{aligned} \left(\mathbf{L}_n + \frac{\Delta t \dot{\mathbf{L}}_n}{2} + \frac{\Delta t(\mathbf{R}_n + \mathbf{K}_n)}{2} + \frac{\Delta^2 t(\dot{\mathbf{R}}_n + \dot{\mathbf{K}}_n)}{2} \right) \mathbf{i}_{n+1} = \\ \frac{\Delta t(\mathbf{e}_{n+1} + \mathbf{e}_n)}{2} + \left(\mathbf{L}_n - \frac{\Delta t \dot{\mathbf{L}}_n}{2} - \frac{\Delta t(\mathbf{R}_n + \mathbf{K}_n)}{2} \right) \mathbf{i}_n. \end{aligned} \quad (8)$$

- Once (8) is solved, force and torque are evaluated again with the corrected values of the currents $\mathbf{i}(t_{n+1})$ just obtained. The integration of the mechanical equations yields the corrected position of the moving body.

The integration method has been validated and the results exhibit a very good accuracy respect to the experimental data found in literature.

IV. SIMULATION RESULTS

We considered a device with an average toroid radius of 8 cm. We performed a set of simulations driving the rotor at different rotational speeds. At low speeds (less than 3000 rpm), we observed a small stabilizing effect; at speed greater than 4000 rpm the magnetic drag force reduces and the stabilizing effect is appreciable. Results correspondent to a speed of 4800 rpm are reported here.

Referring to Fig. 2 (which is not in scale), the red and cyan radial magnetized sectors have an angle of 67.50° , the green and yellow ones have an angle of 45° , while the brown and blue azimuth magnetized sectors have an angle of 33.75° . The radial width is 0.5 cm for the red and yellow sectors, 1 cm for the green and cyan ones, and 0.3 cm for the brown and blue ones. The thickness of the conductive (aluminum) sheet is 2 mm and its average radius is 2.2 cm; the clearance between rotor and stator is 7 mm.

The numerical formulation described in Section 3 has been used to perform the analysis of the described device operating under different conditions.

We started considering the device without the conductive sheet and having an initial position characterized by the rotation shaft x-displacement of 1.5 mm with respect to the symmetry axis.

The results of simulation are shown in Figs. 3 and 4. The levitation force is 450 N. As expected the system is unstable with respect to the radial direction and with respect the rotation around the x and the y axes. The contact between the rotor and the stator happens after about 3 ms.

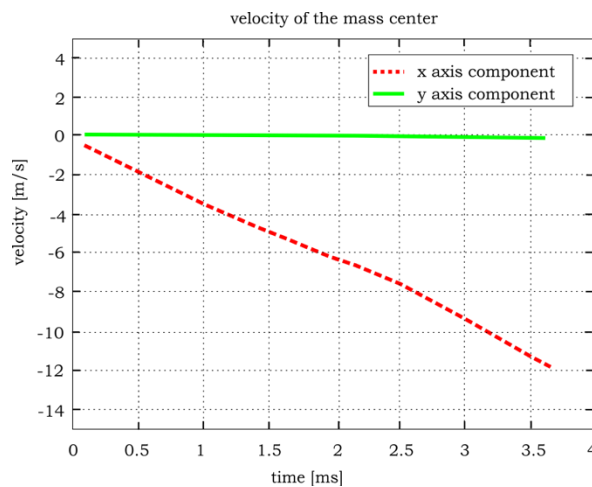


Fig. 3. Velocity of the center of mass of the rotor.

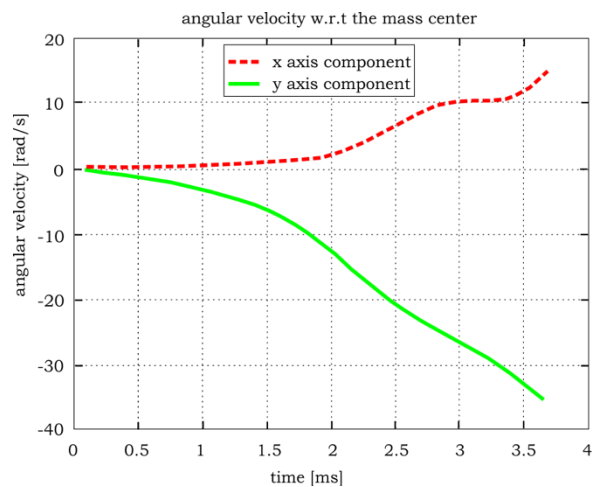


Fig. 4. Components of the angular velocity.

Figures 5 and 6 refer to the configuration with the conductive sheet. The levitation force is raised to 470 N because of the effect of the eddy current. Even in this case the rotor touches the stator because of the unstable

behavior of the system. Comparing the behavior described by Figs. 5 and 6 (presence of the conductive sheet) with the one in Figs. 3 and 4 (absence of conductive sheet), we can see that the eddy currents on the conductive sheet are able to slower the unstable dynamics; the rotor takes a longer time (about 17 ms) to touch the stator. Although the eddy currents are not able to stabilize the device, they can be used to reduce the complexity of the control system. In fact, a lower dynamic requires a slower control action, easier to be designed.

Further simulations have been performed on the device with a reduced number of DOFs preventing rotations with respect to x and y axes.

Figure 7 shows the waveforms of the three components of the velocity of the center of mass of the rotor, while Fig. 8 shows waveforms of the force components; the simulations correspond to the same initial lateral displacement $dx = 1.5 \text{ mm}$.

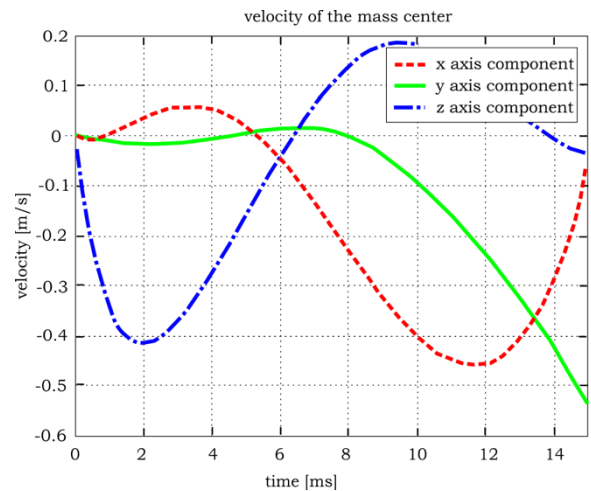


Fig. 5. Velocity of the center of mass of the rotor.

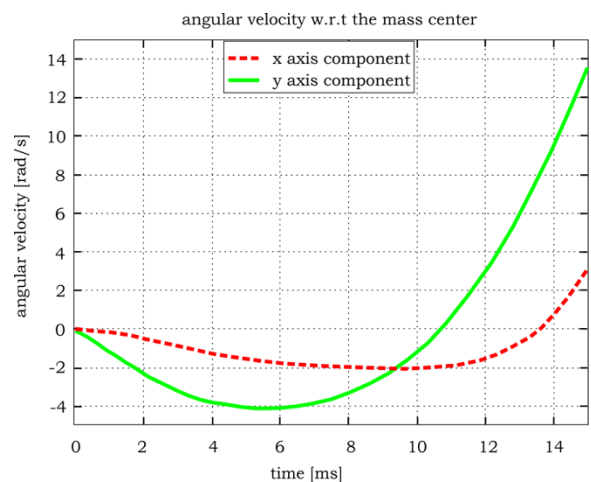


Fig. 6. Components of the angular velocity.

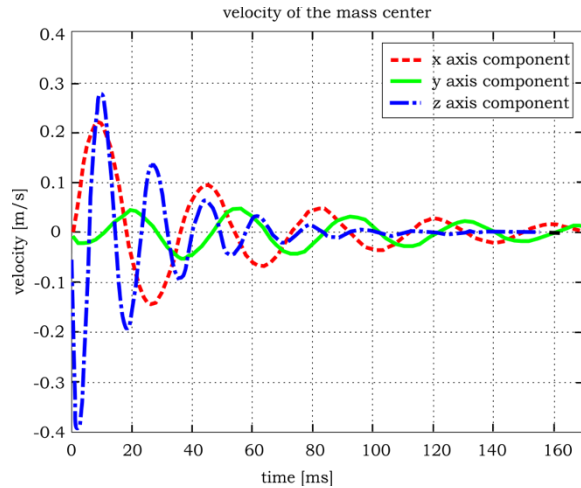


Fig. 7. Velocity of the center of mass of the rotor with 3 DOFs.

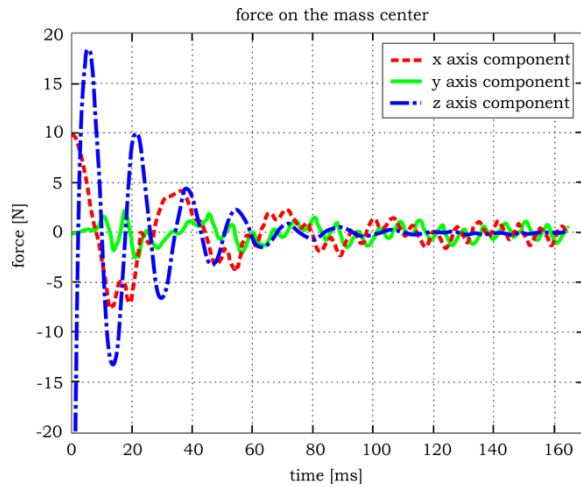


Fig. 8. Force of the center of mass of the rotor with 3 DOFs.

The results of the simulations show that the dynamic of the system is stable. This is actually a good result if we think that in this kind of devices, stability has to be discussed in the contest of dynamics. This means that the robustness requirements previously mentioned, involve concepts of dynamic stability in presence of modeling error due to uncertainties (modern nonlinear dynamics). This theory, usually, not only requires the knowledge of how the forces and torques change with the position and orientation but also of how they changes with both linear and angular velocities. The control systems are consequently usually really complex: this result is then really interesting because it permits a simpler synthesis of the active controller and so reducing the cost. Another similar simulation has been done applying a lateral force of 10 N to the rotor. The results are shown in Figs. 9 and 10; the system is able to compensate the lateral force as

well as for the lateral displacement.

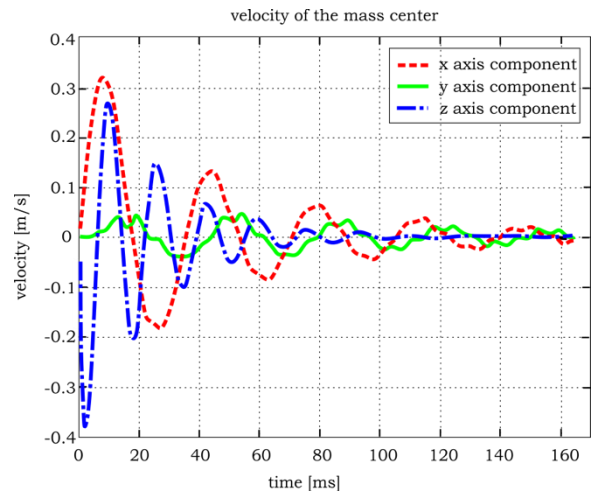


Fig. 9. Velocity of the center of mass of the rotor with 3 DOFs.

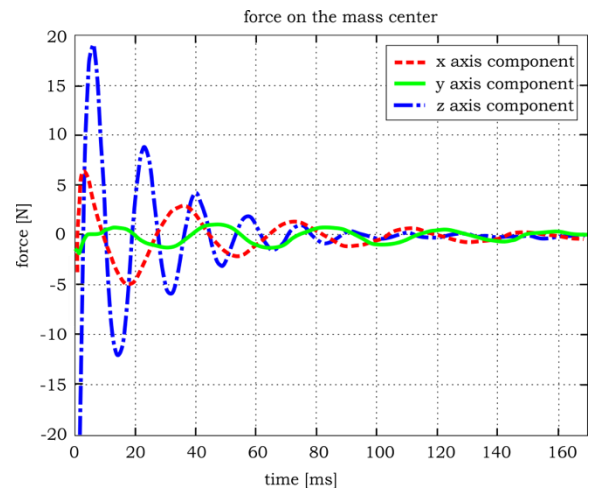


Fig. 10. Force of the center of mass of the rotor with 3 DOFs.

V. CONCLUSIONS

An exhaustive simulation activity has been performed on a PMs bearing based on Halbach array configurations. The conductive sheet is not sufficient to stabilize to system, but it makes slower the unstable dynamics, actually simplifying the control systems action. Since the actuators basically consist of coils, a slower dynamics will need slower control actions, and then smaller voltages. The main result of our analysis relies in the intrinsic stability with respect to the mass center translation, once the rotations with respect x and y axes are prevented. This means that a stabilization system is needed only to maintain the direction of the rotation axis parallel to the z-axis, while the system is able to self-stabilize the position of the rotation axis.

Equivalently, if the stabilizing action results in a net force beside the needed torque, the system is able to compensate this force by adjusting its position.

ACKNOWLEDGMENT

The authors would like to thank the NVIDIA's Academic Research Team for the donation of two NVIDIA Tesla K20c GPUs that have been extensively exploited for the simulations.

REFERENCES

- [1] V. Kozorez and O. Cheborin, "On stability of equilibrium in a system of two ideal current rings," in *Dokl. Akad. Nauk UkrSSR*, Ser. A, vol. 4, pp. 80-81, 1988.
- [2] F. C. Moon, *Chaotic and Fractal Dynamics: Introduction for Applied Scientists and Engineers*. John Wiley & Sons, 2008.
- [3] H.-W. Lee, K.-C. Kim, and J. Lee, "Review of maglev train technologies," *IEEE Trans. Mag.*, vol. 42, no. 7, pp. 1917-1925, 2006.
- [4] J. Meins, L. Miller, and W. Mayer, "The high speed maglev transport system transrapid," *IEEE Trans. Mag.*, vol. 24, no. 2, pp. 808-811, 1988.
- [5] N. Amati, A. Tonoli, F. Impinna, and J. Girardello Detoni, "A solution for the stabilization of electrodynamic bearings: Modeling and experimental validation," *Journal of Vibration and Acoustics*, vol. 133, pp. 021 004-1, 2011.
- [6] A. Tonoli, N. Amati, F. Impinna, J. G. Detoni, H. Bleuler, and J. Sandtner, "Dynamic modeling and experimental validation of axial electrodynamic bearings," in *Proc. of the 12th Int. Symposium on Magnetic Bearings*, pp. 68-73, 2011.
- [7] M. Ono, S. Koga, and H. Ohtsuki, "Japan's superconducting maglev train," *IEEE Instrum. & Measur. Magazine*, vol. 5, no. 1, pp. 9-15, 2002.
- [8] E. Diez-Jimenez, J.-L. Perez-Diaz, and J. C. Garcia-Prada, "Local model for magnet-superconductor mechanical interaction: Experimental verification," *Journal of Applied Physics*, vol. 109, no. 6, (063901), 2011.
- [9] M. Ceraolo, G. Lutzemberger, and D. Poli, "Aging evaluation of high power lithium cells subjected to micro-cycles," *Jour. of Energy Storage*, vol. 6, pp. 116-124, 2016.
- [10] S. Barsali, M. Ceraolo, R. Giglioli, and D. Poli, "Storage applications for smartgrids," *Electric Power System Research (EPSR)*, vol. 120, pp. 109-117, Mar. 2015.
- [11] A. Musolino, R. Rizzo, M. Tucci, and V. M. Matrosov, "A new passive maglev system based on eddy current stabilization," *IEEE Trans. Mag.*, vol. 45, no. 3, pp. 984-987, 2009.
- [12] A. Musolino, M. Raugi, R. Rizzo, and E. Tripodi, "Stabilization of a permanent-magnet MAGLEV system via null-flux coils," in *IEEE Trans. on Plasma Sci.*, vol. 43, no. 5, pp. 1242-1247, 2015.
- [13] S. Earnshaw, "On the nature of the molecular forces which regulate the constitution of the luminiferous ether," *Trans. Camb. Phil. Soc.*, vol. 7, pp. 97-112, 1842.
- [14] K. Halbach, "Application of permanent magnets in accelerators and electron storage rings," *Journal of Applied Physics*, vol. 57, no. 8, pp. 3605-3608, 1985.
- [15] S. Barmada, A. Musolino, M. Raugi, and R. Rizzo, "Analysis of the performance of a combined coil-rail launcher," *IEEE Trans. Mag.*, vol. 39, no. 1, pp. 103-107, Jan. 2003.
- [16] A. Musolino, M. Raugi, and B. Tellini, "3-D field analysis in tubular induction launcher with armature transverse motion," *IEEE Trans. Magn.*, vol. 35, no. 1, pp. 154-159, Jan. 1999.
- [17] R. Albanese, M. Canali, A. Musolino, M. Raugi, G. Rubinacci, and S. Stangherlin, "Analysis of a transient nonlinear 3-D eddy current problem with differential and integral methods," *IEEE Trans. Magn.*, vol. 32, no. 3, pp. 776-779, May 1996.
- [18] E. Tripodi, A. Musolino, R. Rizzo, and M. Raugi, "A new predictor-corrector approach for the numerical integration of coupled electromechanical equations," *Int. J. for Num. Meth. in Eng.*, vol. 105, no. 4, pp. 261-285, 2016.
- [19] S. Quondam Antonio, A. Faba, G. Carlotti, and E. Cardelli, "Vector hysteresis model identification for iron-silicon thin films from micromagnetic simulations," *Physica B: Condensed Matter*, vol. 486, pp. 97-100, 2016.
- [20] S. Barmada, A. Musolino, M. Raugi, and R. Rizzo, "Analysis of the performance of a multi-stage pulsed linear induction launcher," in *IEEE Trans. on Magn.*, vol. 37, no. 1, pp. 111-115, Jan. 2001.
- [21] A. Musolino, R. Rizzo, and E. Tripodi, "The double-sided tubular linear induction motor and its possible use in the electromagnetic aircraft launch system," in *IEEE Trans. on Plasma Sci.*, vol. 41, no. 5, pp. 1193-1200, 2013.
- [22] A. Musolino, R. Rizzo, and E. Tripodi, "Tubular linear induction machine as a fast actuator: Analysis and design criteria," *Progress In Electromag. Research*, vol. 132, pp. 603-619, 2012.
- [23] A. Musolino, R. Rizzo, and E. Tripodi, "Travelling wave multipole field electromagnetic launcher: An SOVP analytical model," in *IEEE Trans. on Plasma Sci.*, vol. 41, no. 5, pp. 1201-1208, 2013.